

Computer vision for nanoscale imaging

Eraldo Ribeiro · Mubarak Shah

Received: 11 February 2006 / Accepted: 11 February 2006 / Published online: 9 June 2006
© Springer-Verlag 2006

Abstract The main goal of Nanotechnology is to analyze and understand the properties of matter at the atomic and molecular level. Computer vision is rapidly expanding into this new and exciting field of application, and considerable research efforts are currently being spent on developing new image-based characterization techniques to analyze nanoscale images. Nanoscale characterization requires algorithms to perform image analysis under extremely challenging conditions such as low signal-to-noise ratio and low resolution. To achieve this, nanotechnology researchers require imaging tools that are able to enhance images, detect objects and features, reconstruct 3D geometry, and tracking. This paper reviews current advances in computer vision and related areas applied to imaging nanoscale objects. We categorize the algorithms, describe their representative methods, and conclude with several promising directions of future investigation.

1 Introduction

In this paper, we review the state-of-the-art of computer vision and related areas applied to imaging applications at the nano scale. Nanotechnology allows us to

understand unique properties of matter at atomic and molecular level spanning a wide range of applications in areas such as medicine, micro-processor manufacturing, material sciences, and environmental technologies. The use of image-based characterization techniques are essential to nanoscale research, and the role of image analysis has considerably expanded over the past few years. Visual inspection of defects, particle selection, and analysis of three-dimensional (3D) structure are few examples of tasks performed with the help of images in nanoscale sciences. We believe that nanoscale image-based characterization represents a novel and rich field of application for both computer vision and image processing technologies. Current development in computer vision algorithms in object recognition, 3D reconstruction, filtering, and tracking represent a small sample of the many potential applications of computer vision research that can be applied to nanoscale imagery.

Traditional computer vision algorithms analyze images generated by the interaction of visible light with the observed scene. In nanoscale characterization, images are mostly created by measuring the response of electrons on the material's surface as they interact with emitted electron beams and atomic size probes. This non-conventional acquisition process poses several challenges to traditional computer vision methods. Most of these challenges are due to the type of imaging instrumentation required to analyze objects at such a small scale. In the following sections, we summarize some of these main challenging factors:

- *Extremely low signal-to-noise ratio (SNR).* Nanoscale images usually have extremely low signal to noise ratio even when generated by highly sophisticated imaging devices such as the Transmission

E. Ribeiro (✉)
Department of Computer Sciences,
Florida Institute of Technology,
Melbourne 32901, USA
e-mail: eribeiro@cs.fit.edu

M. Shah
Computer Vision Laboratory,
School of Computer Science, University of Central Florida,
Orlando, FL 32826, USA

Electron Microscope (TEM) and Scanning Electron Microscope (SEM). The high level of noise in these images can be considered the major complicating factor for computer vision algorithms.

- *Transparent appearance of specimens.* Nanoscale objects may have transparent appearance (e.g., crystals and biological structures). This transparency creates an extra challenge to algorithms for vision applications such as feature detection, recognition, and 3D reconstruction algorithms.
- *Limited number of images per observation.* The destructive nature of some imaging procedures as well as lengthly image acquisition procedures reduce the number of images that one may use for analysis and training. As a result, computer vision methods will need to train and work on very reduced data sets that will pose further challenges to the algorithms.
- *Complex image formation geometry.* Traditional model (perspective) of imaging formation does not always constitute a reasonable model for nanoscale imaging devices. Orthographic and affine projections are usually considered as reasonable approximations of the imaging geometry of electron microscopy. However, more extensive work is still to be done on modeling the electron image formation process from the computer vision standpoint.

The amount of research on nanoscale imaging analysis has increased considerably in the past 10 years. Recent advances by both computer vision and image processing communities combined with the availability of affordable high-performance computer hardware are making image-based nanoscale characterization an important research field. In this paper, we aim to provide a review of computer vision and image analysis techniques used for nanoscale characterization.

A large amount of the current work in the literature deals with the problem of particle detection. Automatic particle detection is a required step before another main task in nanoscale imaging, the 3D reconstruction of particles, can be performed. These two tasks are closely related as the process of reconstructing the 3D geometry of individual particles requires a large number of images taken from varying angles. In some applications, the required number of particles to produce reasonable 3D models can be as large as tens of thousands. 3D modeling of nanoscale objects is another active area of research. Finally, image enhancement and virtual reality applications are other popular topics.

In this paper, we focus mainly on the application of computer vision to images of objects at a typical scale of less than 100 nm. Images of objects of such a small scale are produced by electron microscopy such as the

scanning electron microscope and the transmission electron microscope. However, some of the approaches discussed in this paper can also be applied to larger-scale objects. For instance, optical and fluorescence microscopy represent two other fields with plenty of applications for computer vision algorithms. However, these methods will not be discussed in this paper, as the resolution of fluorescent microscope is the same as their optical counterparts. Fluorescent microscopy allows for the characterization of in-vivo biological specimens that can be processed [77], reconstructed in 3D [69], and tracked [7,9].

The remainder of this paper is organized as follows. Section 2 reviews the most common imaging instruments used for characterization of nanoscale objects. Section 3 provides a taxonomy of the methods. We conclude in Sect. 4 by summarizing a few directions for future computer vision research in this new and exciting field of application. As in any new area of research, there is a large number of problems to be addressed.

2 Nanoscale imaging devices

In this section, we provide a brief description of the most commonly used nanoscale imaging devices. In order to develop effective image-analysis algorithms it is important to understand the basic principles behind the image formation for each instrument. A more detailed description of the optics and physical principles used in electron microscopy can be found in [29,32,87]. Nanoscale images are often obtained by measuring the level of energy produced by the interaction of electrons on the specimen's surface with a beam of electrons emitted by the microscope. This is the basic essence of imaging devices such as scanning electron microscopy (SEM) and transmission electron microscopy (TEM). Images at the nanoscale are also obtained by measuring the reactive force resulting from the interaction of a nanoscale mechanical stylus-like probe with the specimen's surface. Atomic force microscopy (AFM) is an example of such a technique. In Fig. 1 we illustrate the visualization range for the currently available major microscopes along with examples of structures that are visualized at those scales. For comparison purposes, the figure also includes examples of the resolution range achieved by light microscopy.

In this paper, we focus on images produced by electron microscopy (i.e., TEM[87], AFM [50] and SEM[29, 87]), as they are the main visualization devices used in current nanotechnology characterization. Figure 2 shows examples of images taken using the three types of microscopes. Below we briefly describe each of them.

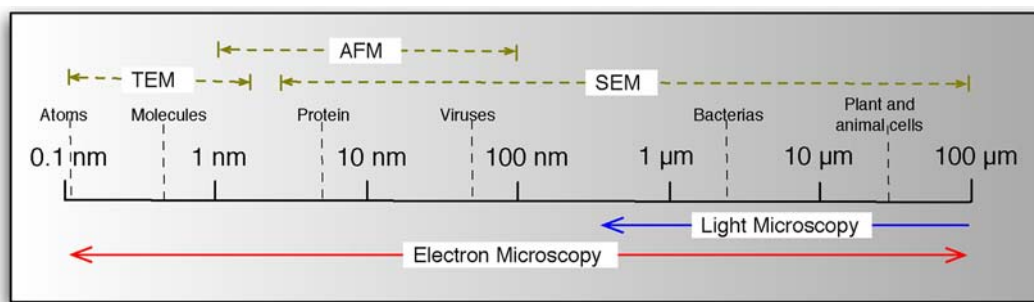


Fig. 1 Visualization scale of nanoscale imaging devices and examples visualized at specific scales (Adapted from [25])

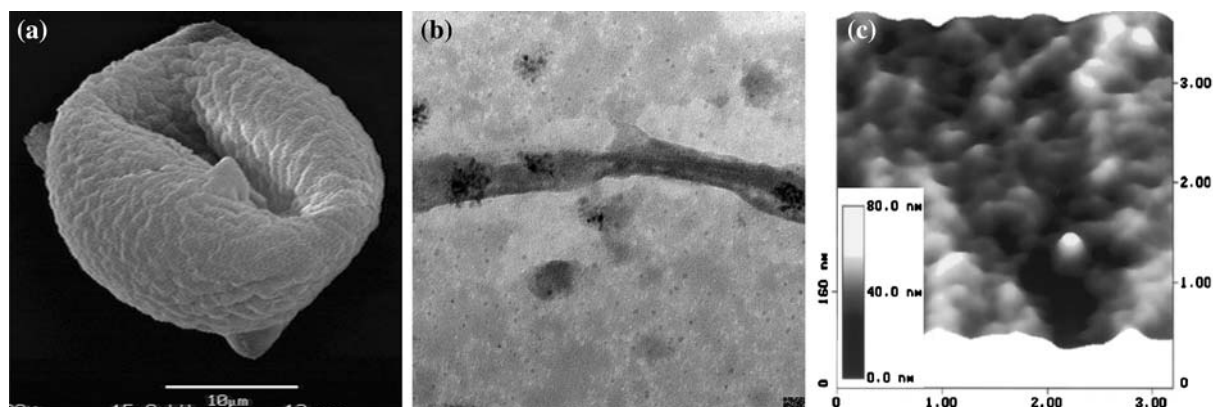


Fig. 2 Electron microscope images. **a** SEM image of a pollen grain. **b** TEM image of a nanotube. **c** AFM image of the surface of living cell (Image from [34])

Scanning electron microscopy Scanning electron microscopies construct an image of an object by detecting electrons resulting from the interaction of a scanning focused-electron beam with the surface of the object operating in high vacuum. The samples of the analyzed material are required to be conductive, as insulated samples will produce distorted images. As a result, samples are often coated with a thin layer of metal (e.g., gold coating). The resolution limit depends mainly on the beam spot size and it can be as small as 1 nm. A common imaging problem in SEM is the possible reaction of the gas with the beam spot due to possible residuals from diluted gas that remains in suspension inside the SEM chamber. This reaction considerably limits the imaging time for true nanoscale objects and often causes a SEM imaging session to produce only a single noisy image of the observed object. Figure 2a shows an example of a SEM image from a pollen grain. SEM images are 2D projections of the 3D imaged specimens. The resulting pixel intensity approximately obeys the inverse of Lambert's law [52], which states that the flux per unit solid angle leaving a surface in any direction is proportional to the cosine of the angle between that direction and the normal to the surface [41].

Transmission electron microscopy Transmission electron microscopy can be considered the most powerful and truly atomic resolution imaging method currently available. It differs from SEM by its sophisticated optics and a very small high-energy power beam of electrons that passes through the sample. Transmittance through samples is required so that the microscope can achieve visualization at the atomic level. When compared with conventional optical scale images, transmission microscopy images can have considerably low contrast and extremely low signal-to-noise ratios (SNR). These are the main problems for surface characterization of true nanoscale specimens. The imaging process can be time consuming, and tedious manual tuning results in a limited number of images of each specimen. In Fig. 2b, a carbon nanotube is imaged using TEM along with a few individual particles.

Atomic force microscopy This microscope follows the principle of traditional stylus-based mechanical profilometers [50]. It uses a sharp-tipped micro cantilever mounted on a probe tip of the microscope. The probe tip scans the surface of the sample object and a laser beam measures the probe's deflections. AFM images are

Table 1 Nanoscale imaging instruments

Instrument	Data type	Typical resolution	Key points
SEM	2D	3–7 nm	Non-metallic samples require metallic sputtering Inverse Lambertian reflectance
TEM	2D	0.10–1 nm	Demanding sample preparation Damaging to biological samples Low signal-to-noise-ratio
AFM	3D	1–100 nm	Spatial resolution limited by size and shape of probe tip

Table 2 Categorization of computer vision methods for nanoscale imagery

Approach	Representative Work
Image enhancement and noise removal	Anisotropic diffusion [8,76,77] Structured illumination for super-resolution [31,73]
Particle detection	Template correlation [63] Detecting edges [37,92,94,95] Gray level intensity statistics [79,91] Appearance-based recognition [58,96] Neural networks [65]
3D reconstruction	Multiple-view geometry [12,13,42] Tomographic projection reconstruction [28,43,60,74,81,85] Snakes-based stereo reconstruction [44]
Visualization	Multi-modal registration for visualization [22,23,78]

similar to range images (i.e., surface depth or topography) and resolution is mostly limited by the finite curvature of the tip. Unfortunately, deflection of the probe tip accounts for the interaction of large number of atoms, rendering atomic definition unreliable. AFM is capable of better than 1 nm lateral resolution on ideal samples and of 0.01 nm resolution in height measurements. The 3D surface generated by this microscope does not provide information about the 2D texture on the analyzed surface as does SEM. An example of a surface obtained using AFM is shown in Fig. 2c.

Other available methods for nanoscale imaging include Near-field scanning optical microscopy (NSOM) [68], that uses a sub-wavelength light source as a scanning probe, and the superconducting quantum interference device (SQUIDs) that measures magnetic responses at the nanoscale [30]. New methods for characterization of nanoscale structures are also being developed [40,71].

In general, the quality and resolution of images produced by nanoscale characterization devices depend on various factors, including the nature of the imaged object and the device characteristics. Table 1 summarizes the information in this section. Low SNR and reduced number of images are the main limiting factors for the direct application of computer vision methods to these images. In the next section, we describe current applications of computer vision methods to nanoscale imagery.

3 Computer vision methods for nanoscale images

In this section, we categorize and review existing work on nanoscale imaging in the computer vision literature. Current computer vision methods for nanoscale characterization mostly deal with four main applications listed below:

1. *Image enhancement and noise reduction.* Low resolution images with high levels of noise represent a major problem in nanoscale characterization. Anisotropic diffusion methods appear to be the most suitable for filtering noisy nanoscale images. These methods successfully filter noise while preserving relevant edge details in an image.
2. *Particle detection.* Automatic detection is a required pre-requisite for 3D shape reconstruction of particles. Accurate modeling requires the identification of thousands of particles. This application is of primary importance in Structural Biology.
3. *Three-dimensional reconstruction.* SEM and TEM images are inherently 2D projections of 3D samples. The reconstruction of the observed object is typically achieved in two main ways: tomographic-like reconstruction from projections and multiple-view geometry reconstruction based on epipolar geometry constraints.

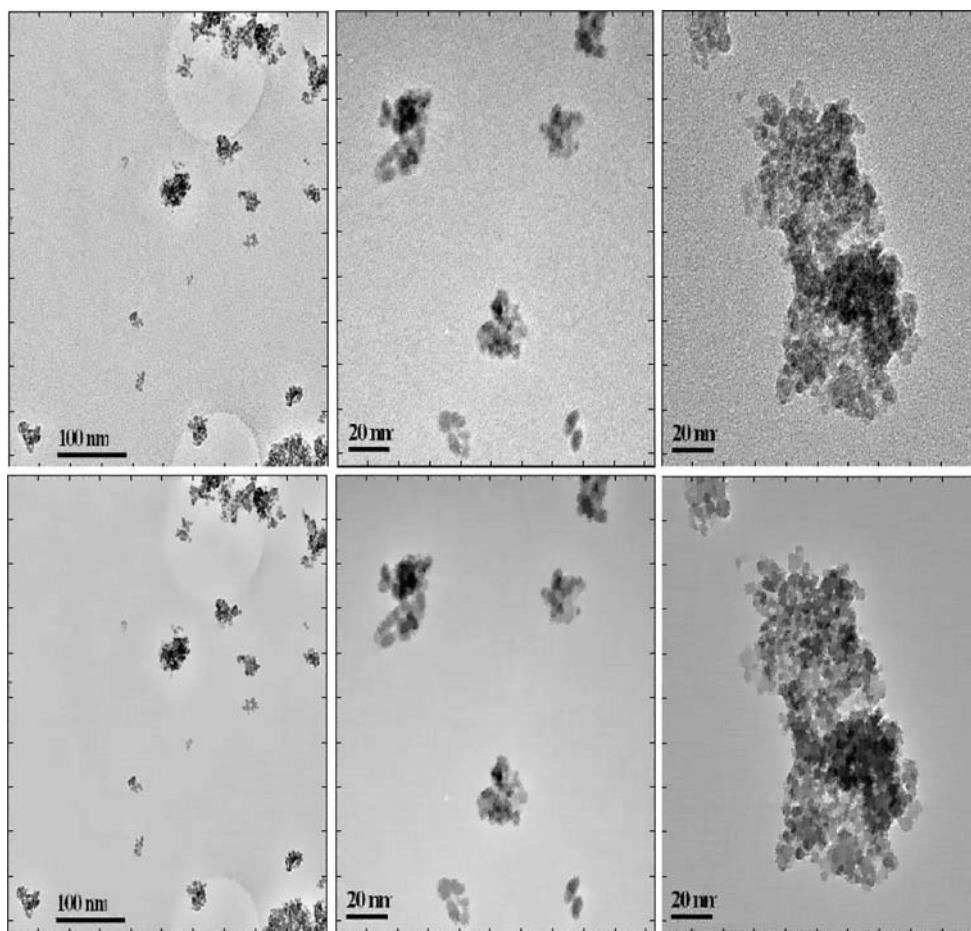


Fig. 3 Example of noise removal in TEM images using anisotropic diffusion. *Top row* original noisy images. *Bottom row* filtered images

4. *Visualization.* Methods for visualization and virtual reality applications at the nanoscale are strongly related to computer vision techniques such as online tracking, image fusion, and image-based rendering. Integration of computer vision and virtual reality can support several aspects of nanoscale characterization.

Table 2 summarizes algorithms and lists representative papers on the application of computer vision techniques

3.1 Image enhancement and noise removal

One of the major challenges in analyzing images of nanoscale objects is the extremely low SNR present in the images even when highly sophisticated imaging devices are used. Addressing this noise problem is a complex task as traditional filtering algorithms work by attenuating high-frequency content and may cause blurring of relevant details in the image [10]. Ideally,

we would like to preserve relevant image-edge information while removing undesirable noise. Techniques such as anisotropic diffusion [67,88] are ideal candidates to handle this type of problem. Anisotropic diffusion allows for the inclusion of an edge-stopping function that controls the level of smoothing across relevant image details. The classic filtering equation as proposed by Perona and Malik [67] can be defined by the following partial differential equation:

$$\frac{\partial I(x, y, t)}{\partial t} = \text{div}[g(\|\nabla I\|)\nabla I], \quad (1)$$

where $\|\nabla I\|$ is the gradient magnitude of the image and $g(\|\nabla I\|)$ is an edge-stopping function that slows the diffusion across edges. An example of an edge-stopping function is $g(x) = 1/(1 + x^2/K^2)$ for a positive K [67]. In Fig. 3, we display results using this method [67] on two TEM images. The top row shows three noisy images of nanoparticles. The bottom row shows the filtered versions of each image after performing diffusion-based noise cleaning. The edges are preserved while the noise

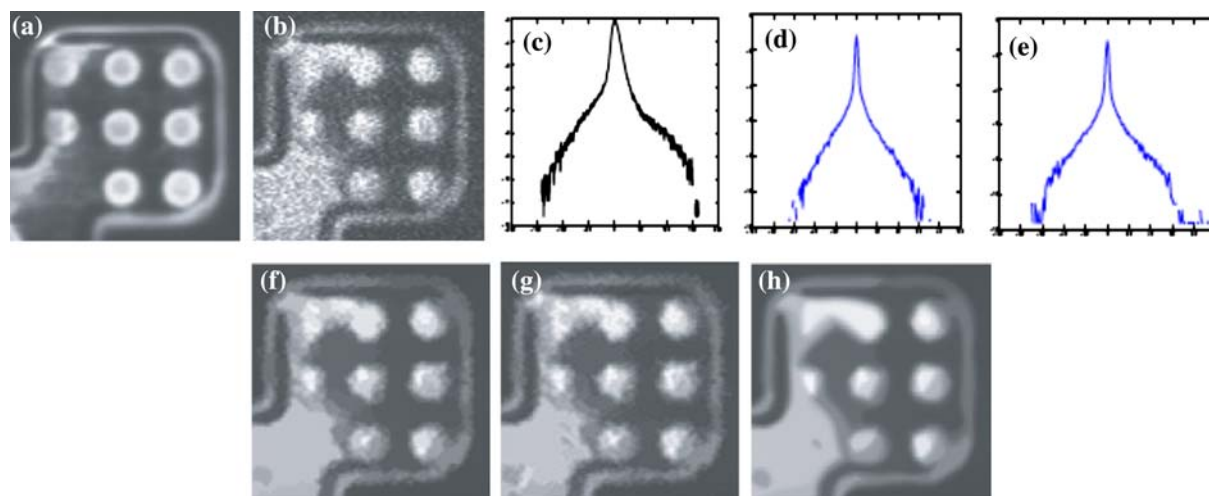


Fig. 4 Empirical distributions. **a** High-quality image (ground truth). **b** Low-quality image. Log distribution of intensity differences ($f_i - g_i$). **c** Log distribution of horizontal edges of the high-quality image. **d** Log distribution of the high-quality image. (All images from [75])

content is removed. This is a very important feature for noise cleaning algorithms in nanoscale imaging as the accuracy of edge location and particles shapes are essential.

Recently published work demonstrates the potential of these techniques on images of nanoscale objects [8, 76]. The most representative work on filtering nanoscale images is the work of Schar et al. [76,75], that describes a diffusion-based method for enhancing silicon device images. Diffusion-based methods are well suited for noise removal in low-quality nanoscale images. One of the main advantages of this technique is that parameters of robust image statistics can be learned from examples. Anisotropic diffusion and its relationship to robust statistics is described in [8].

The method proposed by Schar et al. [75,76] works by creating a statistical model of the noise characteristics and using this model as prior knowledge for reducing noise in low quality images of silicon devices. The idea is to create prior distribution models for both noise and desired features (edges). The parameters of these distributions are estimated by comparing image statistics from samples of both low and high quality images of a given imaging device (e.g., SEM, TEM) and the observed material (e.g., silicon device). Their method is based on the statistical interpretation of anisotropic diffusion [8], as it allows for a mechanism to automatically determine what features should be considered as outliers during the filtering process. Additionally and most importantly, the robust statistics framework allows for the inclusion of spatial and noise statistics as con-

straints which can be used to improve continuity of edges and other important features in the images.

As we mention earlier in this text, the process required to acquire high-quality images of nanoscale objects can be both time consuming and destructive. As a result, it is usually preferable to work with lower-quality images. Thus, noise cleaning algorithms are essential for this type of data. Schar et al. [75] assumes an additive generative model for the pixels in the noisy image such that $f_i = g_i + \eta$, where f_i is the intensity of a pixel in the low-quality image, g_i is the intensity of a pixel in the ground truth image, and η is the noise value originated from an unknown distribution. It turns out that an empirical estimation of the distribution can be obtained from the difference between the high- and the low-quality ones. Figure 4a,b show an example of a high-quality and a low-quality image of a silicon circuit board. Figure 4c,d shows the distributions of gray level intensity differences between two images (a) and (b), and the log distribution of the horizontal edges (a) and vertical edges (b), respectively.

The next step is to fit known distribution models to the estimated empirical distributions. Schar et al. [75] use an adapted version of a recently-proposed model for computing the statistics of images of man-made scenes [53]. Recent work on modeling the statistics of both natural and man-made images is likely to play an important role on the development of new methods for enhancing the quality of nanoscale images [33,39,53]. Following [53], Schar et al. [75] propose the use of t -distribution perturbed by Gaussian noise. The image

is represented by a mixture model [61] in which the first term captures the image edge statistics and the second term captures the image noise:

$$p(X = x) = \frac{w}{Z} \left(1 + \frac{x^2}{\sigma_1^2}\right)^{-t} + (1 - w) \frac{1}{\sqrt{2\pi}\sigma_2} \exp\left(-\frac{x^2}{2\sigma_2^2}\right). \quad (2)$$

In Eq. 2, X is a random variable representing an edge filter response for the image (data difference, horizontal and vertical derivatives), $0 \leq w \leq 1$ represents the mixture proportions of the two terms, and Z is a normalization factor that ensures that the integral of the first term of the equation is 1. Based on the previous assumptions, the image recovering problem can be cast as the maximum a posteriori estimation problem:

$$p(\mathbf{g}|\mathbf{f}) = \prod_i (p(f_i|g_i) \prod_{j=1}^J p(\mathbf{n}_j \nabla g_i)), \quad (3)$$

where $p(f_i|g_i)$ is defined by the measured image statistics, and $p(\mathbf{n}_j \nabla g_i)$ is a spatial prior in terms of local neighborhood derivatives. The maximization of Eq. 3 is achieved using the standard minimization of the negative logarithm. Scharr et al. [75] also propose the use a B-spline approximation of the likelihood function and apply a gradient descent to estimate the parameters of that function. The B-spline model is a robust statistics kernel $\rho(x)$ that allows the problem to be converted to a robust statistics anisotropic diffusion of the following form:

$$E(g, \nabla g) = \int_{\Omega} \rho_0(g(\mathbf{x}) - f(\mathbf{x})) + \lambda \sum_{j=1}^J \rho_j(|\mathbf{n}_j \nabla_{\sigma} g(\mathbf{x})|) d\mathbf{x}, \quad (4)$$

where \mathbf{x} is a pixel location in the image domain Ω . Figure 4f–h show some of the results produced using this method. The above framework can be directly extended to the multidimensional case. Scharr and Uttenweiler [77] demonstrate the application of the 3D extension of the diffusion filtering to the problem of enhancing time-varying fluorescence microscopy images of Actin filaments.

The combination of robust statistics and anisotropic diffusion can be considered as one the most effective methods to enhance the quality of noisy nanoscale images. The framework is also promising if coupled with other computer vision techniques such as object recognition and image segmentation. The use of prior knowledge can be extended by employing more advanced models for spatial interaction [49] rather than simply

representing the priors by means of 1D frequency distributions of edge directions.

3.2 Automatic particle detection

The ability to automatically detect particles in TEM images is essential in cryo-electron microscopy [62,96]. Detecting single particles represents the first stage of most 3D single particle reconstruction algorithms [28, 81,60]. Usually, a typical particle 3D reconstruction process would necessarily need to use thousands of or even millions of particles to produce a reasonable 3D model. This alone makes manual interaction for particle selection unfeasible and practically impossible. In the literature, the problem of particle selection is by far the most studied problem in nanoscale computer vision. A recent comparison of particle detection algorithms for TEM images is presented by [96], and an overview of current methods can be found in [62].

Methods for particle detection in TEM images can be broadly grouped into two main classes: non-learning methods and learning methods. Next, we summarize the two approaches.

3.2.1 Non-learning methods

The main characteristic of non-learning methods is that they do not require a training or learning stage. Methods in this group include approaches based on template correlation [4,68,80], edge detection [37,92,95], and gray level intensity [79,91]. However, non-learning methods tend to be less flexible and sensitive to both noise and small variations in particle appearance when compared to other approaches (Fig. 5)

Particles in micrograph images tend to have very similar appearance, and sometimes can be assumed to appear in a reduced number of poses. If the appearance and size of the particles do not change, template-matching algorithms [14] can help determine the location of the particles. Template matching based on cross correlation [11] is one of the mostly used methods for object detection in images. It works by calculating a matching score between a template image and an input image that contains instances of the objects to be detected. The cross correlation between a template $g(x, y)$ and an image $f(x, y)$ is given by:

$$f(x, y) \oplus g(x, y) = \int f(x, y)g(x + \alpha, y + \beta)d\alpha d\beta, \quad (5)$$

where α and β are dummy variables of integration. Correlation-based approaches for particle detection work well when the location of the object is determined mostly by an unknown translation. However, techniques

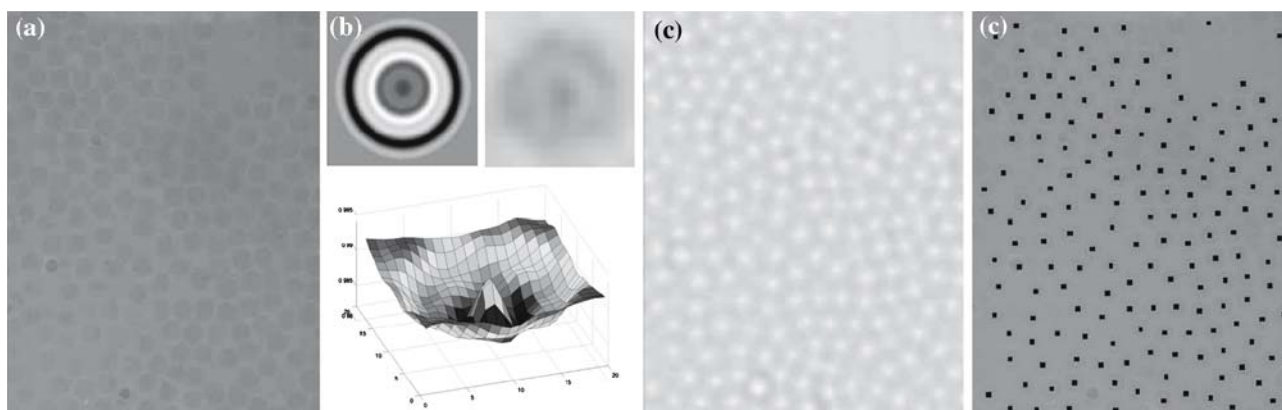


Fig. 5 Detecting particles using correlation-based approach. **a** Original micrograph image. **b** Template for matching and 3D surface plot of the correlation peak. **c** Correlation response on entire image. **d** Detected particles (All images from [4])

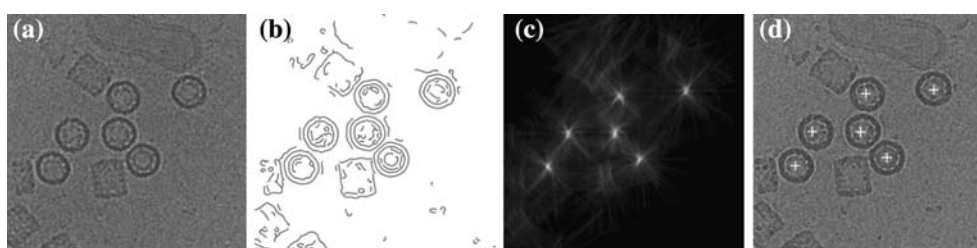


Fig. 6 Detecting circular particles using an edge-based Hough transform approach [95]. **a** Original micrograph image. **b** Detected edges. **c** Accumulation space of Hough transform. **d** Detected particles (All images from [95])

usually generate a large number of false positives, creating the need for manual intervention. Image noise also represents a challenge for correlation-based methods and filtering is usually required before correlation takes place (Fig. 5).

Some particle detection uses edge-detection techniques [37,92,95]. The process consists of detecting edges in the micrograph images. The detected edges are grouped into a shape model used to detect the particles. Examples of such methods include the use of distance transform and Voronoi diagrams [92], and robust voting-based methods such as Hough transforms [95]. Hough transform-based methods work by accumulating edge angle information in a polar coordinate system [21]. The peaks of the polar accumulation space represent the coordinates of the center location of each individual particle. Figure 6 summarizes the process of particle selection described in [95]. In the Figure, (a) shows the original image where particles are to be detected, (b) displays the edge map estimated using an edge-detection technique, (c) shows the Hough accumulation space (highly-voted locations are shown as brighter points), and (d) shows the final detected particles. The Hough transform allows for the detection of any generic shapes, circles and rectangles are the simplest ones.

Analysis of the geometric arrangement of edge information has been used by Yu and Bajaj [92]. The authors describe a particle-detection algorithm that works by fitting Voronoi diagrams [2] to the distance transform [36, 70] of an edge map. The method allows for the detection of rectangular and circular particles in micrographs. The strong reliance on edge-map information makes the method sensitive to noise. To minimize the effects of noise, the authors suggest the use of filtering techniques such as anisotropic diffusion [67,88].

Particles in micrographs tend to have an overall dark appearance when compared to the noisy image background. Information on the homogeneity of pixel gray level intensity may also be used for particle detection. The key idea is to detect individual regions that have specific concentrations of darker pixels. Yu and Bajaj [91] proposed a gravitation-based clustering algorithm that is similar to mode-finding algorithms such as the mean shift [17]. The gravitation-based algorithm assumes that particles represent disconnected regions of low pixel intensity. Detection is accomplished by clustering these regions followed by consistency tests to eliminate false positives connected particles.

Singh et al. [79] proposed a particle detector based on clustering regions containing pixels of low intensity.

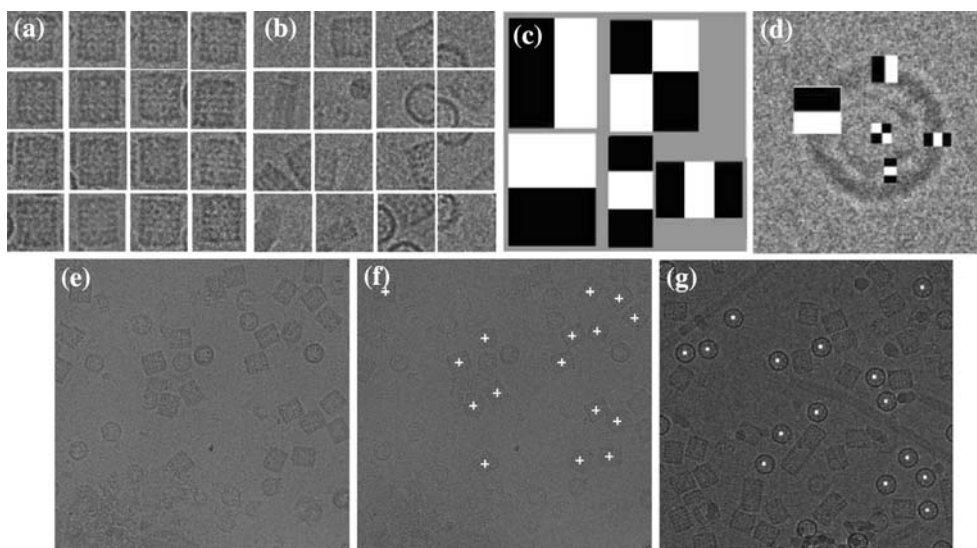


Fig. 7 Detecting particles using learned features. **a** Images of particles. **b** Images of non-particles. **c** Multi-scale, multi-orientation rectangular set of features used for training. **d** Best selected features for detection. **e** Image containing particles to be detected. **f** Detected rectangular particles. **g** Detected circular particles. (All images from [58])

In this case, the authors propose the use of a statistical model of pixel-intensity distribution based on Markov Random Fields [55]. Regions of the micrograph that are likely to contain particles were determined by a segmentation algorithm and the parameters of the Markov Random Field were estimated using the Expectation–Maximization algorithm [19]. However, the detection of the correct location of each particle is a slow process and produces many wrong detections.

The next group of methods use machine-learning techniques to build detectors that are capable of learning the general appearance of the particles.

3.2.2 Learning-based methods

Learning-based methods typically work in a two-stage process [58,96]. The first stage is called learning. During this stage, an appearance model is created from a set of training images of particles. The learned models will allow for the recognition of particles even under variations in appearance and a certain level of image noise. The second stage is the detection stage that consists of scanning the target at every location in the search space for acceptable matches. The location of the best matches will be the location of the detected particles. Methods based on neural networks are also included in this group [65].

The image is scanned for the presence of particles that are similar to the learned model. Methods in this group have the advantage of being both very general (i.e., able to detect particles of any shape) and robust to noise, two critical requirements in TEM image analysis.

As mentioned earlier in this paper, the main problem encountered by current particle detection algorithms is the inherent SNR in TEM images. As a consequence, boundary and shape extraction are hard to accomplish. A second problem is that the shape of the particles may not be geometrically defined, resulting in the need for more complex appearance models. Learning-based algorithms such as the one proposed by Viola and Jones [86] represent a promising way to solve the problem of particle detection under noisy conditions. However, depending on the level of complexity of the objects, the learning stage can be computationally demanding and slow. Additionally, good detection rates depend on the ability of the classifier to learn a representative model for the particles. This usually requires that a large number of features are measured over a large number of training images.

Mallick et al. [58] applies an Adaboost-based learning algorithm to detect particles in Cryo-EM micrographs. Their method works as follows. First, a training set containing images of particles and non-particles is used to train the classifier. This is an off-line process. Once the classifier is trained, an on-line detection process is performed to detect the location of the particles in the micrograph. Figure 7a,b show examples of images from both particle and non-particle training set, respectively. Figure 7c shows the type of features used by the classifier during the training stage. Figure 7d shows the best-performing features determined by the Adaboost learning. Figure 7e–g show a micrograph image and the resulting detected particles (circular and rectangular, respectively).

The detection stage in [58] uses a two-stage cascade classifier. The cascade design aims at speeding the detection process by ruling out most of the non-particle images at the first stage. The second stage makes the final decision if a subregion should be accepted as a particle. The key idea here is that a strong classifier can be built from a linear combination of weak classifiers [86]. In turn, classifier $F(t)$ at each stage is composed of a linear combination of K simple classifiers based on a single feature (weak classifiers). For example, let $f_k(t)$ with $k \in \{1, \dots, K\}$ represent weak classifiers that produce a response $+1$ or -1 for each particle or non-particle subimages, respectively. A strong classifier for a stage of the cascade can be formed as a linear combination of the weak classifiers as follows:

$$F(t) = \begin{cases} +1, & \sum_{k=1}^K \alpha_k f_k(t) \geq \mathcal{T} \sum_{k=1}^K \alpha_k \\ -1, & \text{otherwise,} \end{cases} \quad (6)$$

where $\alpha = (\alpha_1, \dots, \alpha_K)$ is a vector of weights indicating the contribution of each classifier to the final decision and \mathcal{T} is a threshold that determines the tradeoff between false-negative and false-positive rates. The approach consists of training a large number of classifiers $f_k(t)$ using the training sets for particle and non-particle images, and automatically selecting the best candidates of measurements using the Adaboost algorithm. This algorithm selects and combines the best set of simple classifiers $f_k(t)$ to form a strong classifier that achieves close to ideal classification rates. The algorithm uses rectangular features, as they are both fast to compute, and approximate first and second derivatives of the image at a particular scale. It is worth noting that the weak classifiers can be of any form and are usually simple univariate threshold-based functions. The strength of this approach lies in the correct choices of parameters to form the linear combination of weak classifiers achieved via the Adaboost algorithm.

Improvements to this method can be achieved by pre-filtering the images before training and detection. However, in principle the algorithm should work for very noisy conditions as long as the classifier is trained under those same conditions. Additionally, 3D objects under arbitrary poses can represent a problem to this method. Next, we discuss the reconstruction of 3D models of nanoscale structures.

3.3 3D reconstruction of nano-objects

The availability of 3D information is of crucial importance to the analysis of both man-made and biological nanoscale objects. This is especially relevant in fields such as Structural Biology for the development

of detailed structural models and functions of macromolecules[44], and in nanoscale manufacturing processes such as nano-tube fabrication [6,16] that often requires the detection of particles inside and outside of the synthesized nanotubes. A more complete review of tomographic techniques for single particle reconstruction is presented by [85].

As we mentioned in the beginning of this paper, traditional TEM provides only 2D images of objects and, therefore, does not carry any depth information. Tomographic projection reconstruction [28,43,54,60,74,81] and, more recently, multiple-view epipolar geometry [12,13,46] have been effectively applied to the development of methods to provide both depth and structure information of nanoscale objects. We now review some of the works in both categories.

3.3.1 Tomographic reconstruction from projections

Tomographic reconstruction methods are well known techniques in medical applications [72]. The reconstruction of the 3D shape of objects is obtained from the integration of their mapped projections acquired from several viewing angles.

The most frequently used algorithm in this class is the weighted back-projection algorithm [27]. The algorithm has its foundations in the frequency domain theorem, which states that the 2D Fourier transform of a projection through a 3D volume coincides with a plane passing through the origin of the 3D Fourier transform of the volume with the same orientation as the projection. As a result, the Fourier transform of each image can be calculated and placed in the 3D Fourier space based on pre-computed Euler angles that represent the angles of acquisition of each image. Once all Fourier transforms are placed in the 3D Fourier space, the inverse Fourier transform of that space will produce a reconstructed version of the imaged object. The Fourier projection theorem is valid for any dimension. Figure 8a illustrates the 1D projection of a 2D object for a given angle. Figure 8b shows various 2D projections (i.e., images) obtained from a 3D object. Figure 8c shows the reconstruction results for a single nanoscale particle.

The main idea of this method, for the case of reconstructing a 2D object from 1D projections, is summarized as follows. Let us consider the function $f(x, y)$ representing the object of interest. The Fourier transform of f is given by:

$$F(u, v) = \int_{-\infty}^{\infty} \int_{-\infty}^{\infty} f(x, y) e^{-j2\pi(ux+vy)} dx dy. \quad (7)$$

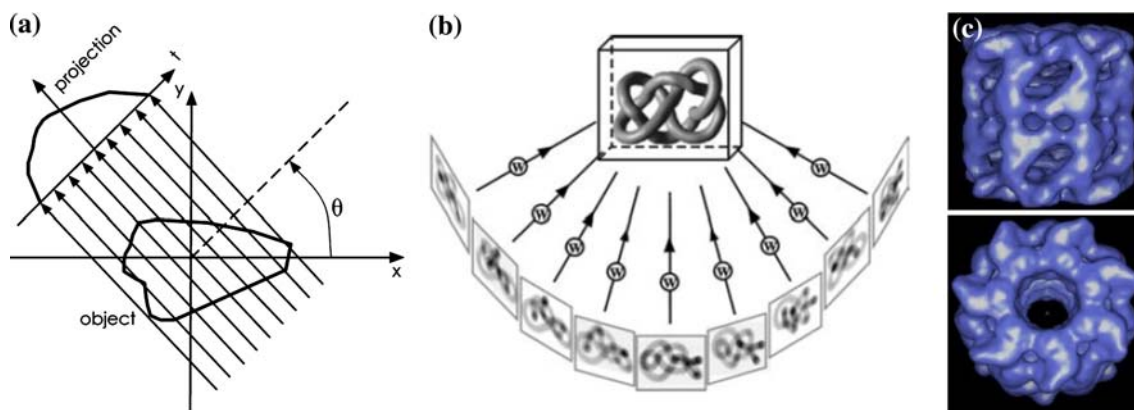


Fig. 8 Reconstruction from angular projections. **a** 1D projection of a 2D object for a given angle θ . **b** Back-projection principle from 2D images to 3D reconstruction (From [57]). **c** 3D reconstruction of nano particles (From [43])

Let $P_\theta(t)$ be the 1D projection of the object image for a given angle θ such that:

$$P_\theta(t) = \int_L f(x, y) dL. \tag{8}$$

As a result, $P_\theta(t)$ is the line integral of the image intensity, $f(x, y)$, along a line L that at a distance $\rho = x \cos \theta + y \sin \theta$. The 1D Fourier transform of the projection is given by:

$$S_\theta(\omega) = \int_{-\infty}^{\infty} P_\theta(t) e^{-j2\pi \omega t} dt. \tag{9}$$

We can now obtain an estimate of $F(u, v)$ from the Fourier transform of various projections from different angles. The reconstructed object is given by the inverse Fourier transform of the angular projections as:

$$f(x, y) = \int_{-\infty}^{\infty} \int_{-\infty}^{\infty} F(u, v) e^{j2\pi (ux+vy)} du dv. \tag{10}$$

The main steps of the algorithm for the 2D case are summarized as follows:

1. Obtain a projection of the object at various angles $\theta_1, \dots, \theta_n$.
2. Calculate the Fourier transform of each projection to obtain $F(u, v)$.
3. Estimate the reconstruction of the object function by calculating the inverse Fourier transform of $F(u, v)$.

However, the reconstruction problem in electron microscopy has many differences from the classical tomography reconstruction of medical images. First, as we mentioned earlier in this paper, electron microscopy

images have very low SNR. Second, the image acquisition process generates a random distribution of projections as the geometry of the data collection cannot be controlled. Finally, gaps in Fourier space are likely to appear due to uneven distribution of projection directions. As a result, in order to produce high resolution reconstructions of the particles, this technique requires the availability of a large number of images of each particle. This is not always possible as TEM image acquisition is an expensive and time-consuming process. Additionally, reconstruction of large molecular biological samples can be computationally demanding, sometimes even requiring the use of special parallel computing hardware [28].

3.3.2 Multiple-view epipolar geometry

Alternatively, computer vision methods for multiple-view reconstruction [26, 38] can effectively be applied to the problem of obtaining 3D models from TEM images. The epipolar geometry constraint [26, 38] allows for the recovery of 3D information from a pair of images of the same scene or object. Recent work by Brandt et al. [12, 13] has demonstrated the application of epipolar geometry for the alignment of multiple TEM images. Epipolar geometry has also been used to perform reconstruction of curved nanowires from SEM images [42], as well as to achieve reconstruction of DNA filaments from TEM images [44]. Cornille et al. [18] describe a calibration algorithm for 3D reconstruction in SEM images.

The alignment of images taken from different viewing angles is a required step before tomographic reconstruction can be performed [85]. The method described by Brandt et al. [12, 13] performs image alignment by means of a global optimization algorithm to solve the feature matching problem over a set of TEM images. Their method starts by finding initial estimates of

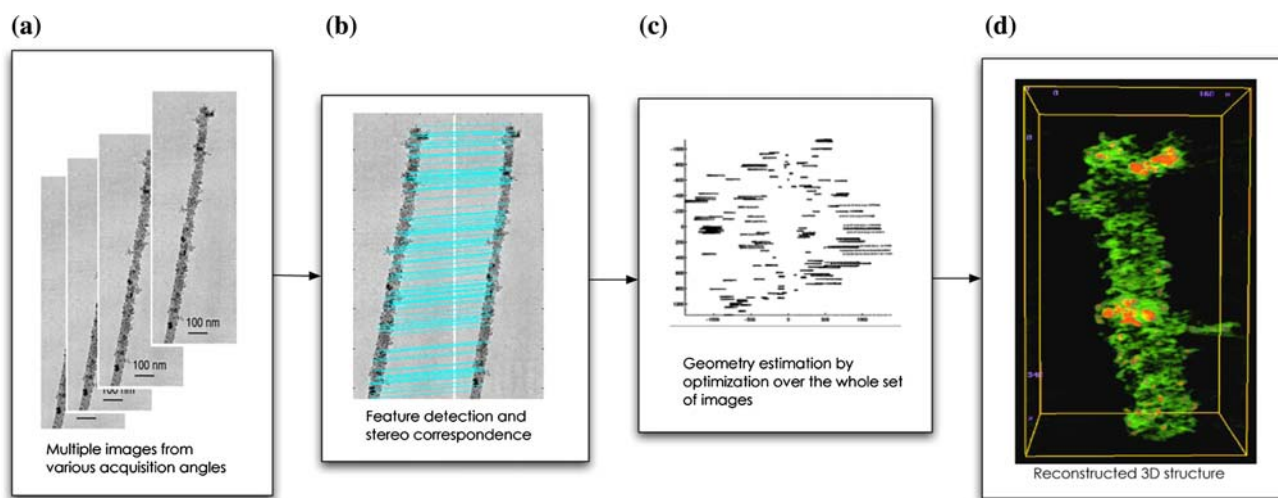


Fig. 9 A TEM 3D reconstruction system from multiple images. Adapted from [12]. **a** A set of images from multiple view points. **b** Frame to frame automatic feature matching. **c** Alignment of the feature tracks using epipolar constraint. **d** Final tomographic reconstruction

feature matches from successive images using the epipolar constraint. This is the stereo matching stage, and it results in a set of point correspondences between each pair of images. Once these corresponding features are at hand, the method solves for the overall image alignment by means of a global optimization algorithm [38]. Finally, the aligned images are used as input for the tomographic reconstruction process. Figure 9 illustrates the process as a sequence of the above mentioned steps.

Jacob et al. [44] proposed a method to achieve reconstruction of DNA filaments from TEM images. The method is based on a spline-snake algorithm that minimizes the 3D to 2D projection error for all views of a cryo-TEM micrographs of a DNA filament. The algorithm requires user initialization of the snake and uses a bank of Gaussian-like directional filters to detect segments of the DNA filament.

Huang et al. [42] describe a method to reconstruct the 3D shape of curved nanowires. The method uses epipolar geometry [26,38] to match stereo pairs of SEM images of nanowires. The image-formation geometry of electron microscopy can be approximated by orthographic projection and parallax motion provides enough information for 3D reconstruction. Segments of the nanowire lying in the epipolar plane cannot be reconstructed. Additionally, the method works better for nanowires with very low curvature.

The reconstruction of nanoscale objects is a promising problem area for computer vision applications. Most work so far has focused on the 3D reconstruction process. However, automatic analysis and recognition of the reconstructed surfaces have not received much attention. Noise and the non-conventional

nature of the source data makes these problems even more challenging and interesting. Next, we present a brief discussion on data visualization and virtual reality methods applied to the problem of nanoscale characterization.

3.4 Visualization and manipulation

Visualization is crucial to nano-technology. Most of the methods described in this section are applications of virtual reality for nanoscale visualization. Virtual reality technology provide an ideal framework to support key applications in nanoscale imaging such as visual inspection of devices for defect detection as well as precise visual-guided manipulation in device manufacturing [35,55,82]. This can be achieved, for example, by fusing multi-modal imaging data and graphics to allow for applications such as device placement and measurement. Additionally, virtual reality also provides excellent means for education and training [66]. A recent review of the applications of virtual reality to nanoscale characterization is presented by Sharma et al. [78].

Fang et al. [24] propose a method for interactive 3D microscopy volumetric visualization. The method consists of a combination of 2D hardware-supported texture mapping and a modified fast volume rendering algorithm based on shear-warp of the viewing matrix [51]. Tan et al. [82] describe a nanoscale manipulator system that works with a scanning-probe microscope (cantilever-based system)(Fig. 10). The system combines force interaction feedback and visualization for nanoscale manipulation through a haptic interface.

Manipulation systems are evolving into immersive virtual reality environments that provide real-time

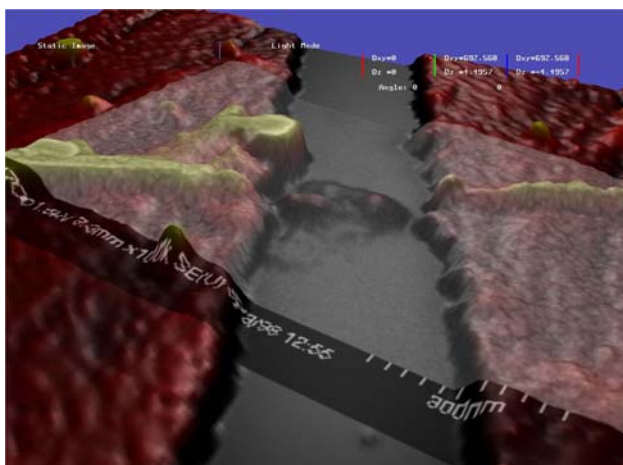


Fig. 10 Broken carbon nano-tube between two raised electrodes [64]

visual and tactile feedback to the users [56]. This allows for the creation of nano-devices and sensors in an environment where users can interact with forces and simultaneously visualize the results of each manipulation.

The development of immersive virtual reality environments is particularly useful in nano-scale manufacturing. This is the direction taken by the Nanoscale Science Research Group at UNC-Chapel Hill. They have developed a nanoscale manipulator system that fuses multi-modal imaging information onto a single visualization output [35]. The system uses projective texture mapping of SEM image onto AFM topography data along with a calibration method that allows for localization of the AFM probe in space. The SEM and AFM datasets are manually aligned and the user can choose the level of relative mixture between the two data sources.

Basic aspects of virtual reality technology are strongly linked to computer vision techniques such as camera calibration [83, 93], augmented reality [3], and real-time video-based tracking [20, 84]. For instance, image-based tracking can, in principle, be used to provide real-time feedback for augmented reality tasks while on-line camera calibration methods allow for 3D alignment of both camera and environment information to support image fusion. Applications such as nanomotion planning of complex manufacturing tasks implies the integration of mechanical haptic systems vision-based global planning, and model-based local motion planing [47].

4 Discussion and conclusions

This paper attempts to provide a comprehensive review of computer vision methods for image-based nanoscale

characterization. The main objective of this paper is to motivate the development of new computer vision algorithms that will address the many challenges in this new and promising application area. We have focused mainly on the characterization and description of the methods without performing quantitative comparisons.

There are several avenues available for future research. Some possible directions include:

- The tracking of particles and surfaces.
- The characterization of noise statistics of nanoscale imaging devices.
- View morphing for visualization when only reduced sets of images are available.
- The development of defect and misalignment detection algorithms.
- The use of texture analysis to characterize nanoscale materials.
- 3D reconstruction using occluding contours and circular motion of the tilting stage.
- The characterization of semi-transparent objects.

Tracking algorithms are often used in many interesting applications [1, 7, 9]. However, tracking is mostly performed at the optical microscope resolution such as fluorescence microscopy for the analysis of biological specimens. At the nanoscale realm we found the work of Mantooth et al. [59], which uses cross-correlation to calculate the drift in scanning tunneling microscope. The algorithm tracks inter-image drift, allowing for registration of a sequence of images into a single coordinate plane. The detection of defects is another important application [48].

Modeling image statistics is key to image enhancing. Following a similar approach as the one proposed by [76], one might attempt to model different levels of noise and image statistics for specific microscopes and material analysis processes (TEM image acquisition). These models can be used to help enhance image quality and analyze device structure. Image enhancement can, in principle, be accomplished through multi-image restoration [16]. This technique is based on the assumption that multiple images of the same object are often corrupted by independently-distributed noise [5]. This allows for image restoration algorithms that combine the information content available in multiple images to obtain a higher quality image output. This can be of help, for example, for TEM imaging when multiple images are available but the individual image quality is poor. In this case, multiple image restoration methods such as the one described in [16] can help produce a better image output.

View-morphing techniques, such as the one developed by Xiao and Shah [89] may help visualization of nanoscale objects by generating novel views of an object from few image samples. The generation of novel views provides a way for creating extra geometrically consistent information without the need for explicit 3D reconstruction. For example, generating TEM images from several view points is a time-consuming and computationally demanding process. View-morphing may reduce the time required for generating novel views by synthesizing geometrically consistent images from few acquired samples.

Tracking [90] and circular motion geometry [45] can be applied to problems such as determining the spatial localization of particles in nanotube fabrication. The key idea is to analyze a sequence of TEM images acquired at varying viewing angles. The main problem here is to determine if particles are present inside or outside of the nanotubes. As TEM images are projections of the 3D objects, it is difficult to determine the exact location of particles in the imaged sample.

Nanoscale imaging is certainly an exciting and challenging field with numerous applications for computer vision research. The low SNR that is a common characteristic of nanoscale images makes the application of vision techniques even more challenging. However, as vision algorithms become more robust and available computer hardware becomes faster, we are able to approach these problems more successfully. In terms of advancing computer vision technology, the challenging aspects of nanoscale image provide an excellent testbed that will drive vision algorithms to become increasingly more robust and accurate.

References

1. Aguet, F., Van De Ville, D., Unser, M.: Sub-resolution axial localization of nanoparticles in fluorescence microscopy. In: Wilson, T., (ed.) Proceedings of the SPIE European conference on biomedical optics: confocal, multiphoton, and nonlinear microscopic imaging II (ECBO'05), vol. 5860, pp. 103–106. Munich, Germany, June 12–16 (2005)
2. Aurenhammer, F.: Voronoi diagrams – a survey of a fundamental geometric data structure. *ACM Comput Surv.* **23**(3), 345–405 (1991)
3. Azuma, R.: A survey of augmented reality. *Presence Teleoperators Virtual Environ.* **6**(4), 355–385 (1997)
4. Banks, J., Rothnagel, R., Hankamer, B.: Automated particle picking of biological molecules images by electron microscopy. In: *Image and vision computing New Zealand*, pp. 269–274, November (2003)
5. Belge, M., Kilmer, M., Miller, E.: Wavelet domain image restoration with adaptive edge-preserving regularization. *Integr. Psychiatry* **9**(4), 597–608 (2000)
6. Bera, D., Kuiry, S.C., McCutchen, M., Kruize, A., Heinrich, H., Seal, S., Meyyappan, M.: In-situ synthesis of palladium nanoparticles-filled carbon nanotubes using arc discharge in solution. *Chem. Phys. Lett.* **386**(4–6), 364–368 (2004)
7. Berglund, A.J., Mabuchi, H.: Tracking-fcs: fluorescence correlation spectroscopy of individual particles. *Opt. Express* **13**, 8069–8082 (2005)
8. Black, M.J., Sapiro, G., Marimont, D., Heeger, D.: Robust anisotropic diffusion. *IEEE Trans Image Process.* **7**(3), 421–432 (1998)
9. Bonneau, S., Dahan, M., Cohen, L.D.: Single quantum dot tracking based on perceptual grouping using minimal paths in a spatiotemporal volume. *IEEE Trans. Image Progress.* **14**(9), 1384–1395 (2005)
10. Bovik, A.C., Gibson, J.D., Bovik, A. (eds.): *Handbook of Image and Video Processing*. Academic, Orlando (2000)
11. Bracewell, R.: *The Fourier Transform and Its Applications* 3rd edn. McGraw-Hill, New York (1999)
12. Brandt, S., Heikkonen, J., Engelhardt, P.: Automatic alignment of transmission electron microscope tilt series without fiducial markers. *J. Struct. Biol.* **136**, 201–213 (2001)
13. Brandt, S., Heikkonen, J., Engelhardt, P.: Multiphase method for automatic alignment of transmission electron microscope images using markers. *J. Struct. Biol.* **133**(1), 10–22 (2001)
14. Brown, L.G.: A survey of image registration techniques. *ACM Comput. Surv.* **24**(4), 325–376 (1992)
15. Chen, Y.K., Chu, A., Cook, J., Green, M.L.H., Harris, P.J.F., Heesom, R., Humphries, M., Sloan, J., Tsang, S.C., Turner, J.F.C.: Synthesis of carbon nanotubes containing metal oxides and metals of the d-block and f-block transition metals and related studies. *J. Mater. Chem.* **7**(3), 545–549 (1997)
16. Chen, Y., Wang, H., Fang, T., Tyan, J.: Mutual information regularized bayesian framework for multiple image restoration. In: *IEEE International conference on computer vision (ICCV)* (2005)
17. Comaniciu, V., Meer, P.: Ker.nel-based object tracking. *IEEE Trans. on Pattern Anal. Mach. Intell.* **25**(5), 564–575 (2003)
18. Cornille, N., Garcia, D., Sutton, M., McNeil, S., Orteu, J.: Automated 3-D reconstruction using a scanning electron microscope. In: *SEM annual conf. & exp. on experimental and applied mechanics* (2003)
19. Dempster, A., Laird, N.M., Rubin, D.B.: Maximum likelihood from incomplete data via the EM algorithm. *J. R. Stat. Soc. Ser. B* **39**(1), 1–38 (1977)
20. Drummond, T., Cipolla, R.: Real-time tracking of complex structures with on-line camera calibration. *Image Vision Comput.* **20**(5-6), 427–433 (2002)
21. Duda, R.O., Hart, P.E.: Use of the hough transformation to detect lines and curves in pictures. *Commun. of ACM.* **15**(1), 11–15 (1972)
22. Falvo, M.R., Clary, G., Helser, A., Paulson, S., Taylor, R.M.II, Chi, F.P., Brooks, V., Jr, Washburn, S., Superfine, R.: Nanomanipulation experiments exploring frictional and mechanical properties of carbon nanotubes. *Micros. Microanal.* **4**, 504–512 (1998)
23. Falvo, M.R., Taylor, R.M., II, Helser, A., Chi, V., Brooks, F.P., Jr, Washburn, S., Superfin, R.: Nanometre-scale rolling and sliding of carbon nanotubes. *Nature* **397**, 236–238 (1999)
24. Fang, S., Dai, Y., Myers, F., Tuceryan, M., Dunn, K.: Three-dimensional microscopy data exploration by interactive volume visualization. *Scanning* **22**, 218–226 (2000)
25. Farabee, M.: On-line biology book. (<http://www.emc.maricopa.edu/faculty/farabee/BIOBK/BioBookTOC.html>) (2001)
26. Faugeras, O.: *Three-dimensional Computer Vision: a Geometric Viewpoint*. MIT Press (1993)

27. Fernandez, J., Lawrence, A., Roca, J., Garcia, I., Ellisman, M., Carazo, J.: High-performance electron tomography of complex biological specimens. *J. Struct. Biol.* **138**, 6–20 (2002)
28. Fernandez, J.-J., Carazo, J.-M., Garcia, I.: Three-dimensional reconstruction of cellular structures by electron microscope tomography and parallel computing. *J. Parallel Distrib. Comput.* **64**(2), 285–300 (2004)
29. Flegler, S.L., Heckman, J.W., Klomparens, K.L.: *Scanning and Transmission Electron Microscopy: An Introduction*. Oxford Press, Oxford (1995)
30. Gallop, J.: SQUIDs: some limits to measurement. *Superconduct. Sci. Technol.* **16**, 1575–1582 (2003)
31. Garini, Y., Vermolen, B.J., Young, I.T.: From micro to nano: recent advances in high-resolution microscopy. *Curr. Opin. Biotechnol.* **16**(3), 3–12 (2005)
32. Goldstein, J.I., Newbury, D.E., Echlin, P., Joy, D.C., Fiori, C., Lifshin, E.: *Scanning Electron Microscopy and X-Ray Microanalysis: A Text for Biologists, Materials Scientists, and Geologists*. Plenum Publishing Corporation, New York (1981)
33. Grenander, U., Srivastava, A.: Probability models for clutter in natural images. *IEEE Trans. Pattern Anal. Mach. Intell.* **23**(4), 424–429 (2001)
34. Grimellec, C.L., Lesniewska, E., Giocondi, M.-C., Finot, E., Vie, V., Goudonnet, J.-P.: Imaging of the surface of living cells by low-force contact-mode atomic force microscopy. *Biophys. J.* **75**, 695–703 (1998)
35. Guthold, M., Liu, W., Stephens, B., Lord, S.T., Hantgan, R.R., Erie, D.A., Taylor, R.M. II, Superfine, R.: Visualization and mechanical manipulations of individual fibrin fibers. *Biophys. J.* **87**(6), 4226–4236 (2004)
36. Haralick, R.M., Shapiro, L.G.: *Computer and Robot Vision*. Addison-Wesley Longman Publishing, Boston, (1992)
37. Harauz, G., Fong-Lochovsky, A.: Automatic selection of macromolecules from electron micrographs by component labelling and symbolic processing. *Ultramicroscopy* **31**(4), 333–44 (1989)
38. Hartley, R.I., Zisserman, A.: *Multiple View Geometry in Computer Vision*. Cambridge University Press, Cambridge, (2000)
39. Heiler, M., Schnörr, C.: Natural image statistics for natural image segmentation. *Int. J. Comput. Vision*, **63**(1), 5–19 (2005)
40. Hell, S.W.: Towards fluorescence nanoscopy. *Nat Biotechnol.* **21**(11), 1347–1355 (2003)
41. Horn, B.: *Robot Vision*. MIT Press, Cambridge, (1986)
42. Huang, Z., Dikin, D.A., Ding, W., Qiao, Y., Chen, X., Fridman, Y., Ruoff, R.S.: Three-dimensional representation of curved nanowires. *J. Microsc.* **216**(3), 206–214 (2004)
43. Ludtke, S.J., Baldwin, P., Chiu, W.: Eman: semiautomated software for high-resolution single-particle reconstructions. *J. Struct. Biol.* **128**, 82–97 (1999)
44. Jacob, M., Blu, T., Unser, M.: 3-D reconstruction of DNA filaments from stereo cryo-electron micrographs. In: *Proceedings of the first 2002 IEEE international symposium on biomedical imaging: macro to nano (ISBI'02)*, vol. II, pp. 597–600. Washington, DC, USA, July 7–10 (2002)
45. Jiang, G., Quan, L., Tsui, H.-T.: Circular motion geometry using minimal data. *IEEE Trans. Pattern Anal. Mach. Intell.* **26**(6), 721–731 (2004)
46. Kammerud, C., Abidi, B., Abidi, M.: Computer vision algorithms for 3D reconstruction of microscopic data—a review. *Microsc. Microanal.* **11**, 636–637 (2005)
47. Kim, D.-H., Kim, T., Kim, B.: Motion planning of an afm-based nanomanipulator in a sensor-based nanorobotic manipulation system. In: *Proceedings of 2002 international workshop on microfactory*, pp. 137–140 (2002)
48. Kubota, T., Talekar, P., Ma, X., Sudarshan, T.S.: A non-destructive automated defect-detection system for silicon carbide wafers. *Mach. Vis. Appl.* **16**(3), 170–176 (2005)
49. Kumar, S., Hebert, M.: Discriminative fields for modeling spatial dependencies in natural images. In: *Proceedings of advances in neural information processing systems (NIPS)*, December (2003)
50. Kumar, S., Chaudhury, K., Sen, P., Guha, S.K.: Atomic force microscopy: a powerful tool for high-resolution imaging of spermatozoa. *J. Nanobiotechnol.* **3**(9), (2005)
51. Lacroute, P., Levoy, M.: Fast volume rendering using a shear-warp factorization of the viewing transformation. In: *SIGGRAPH '94: proceedings of the 21st annual conference on computer graphics and interactive techniques*, pp. 451–458. ACM press, New York, (1994)
52. Lambert, J.H.: *Photometria sive de mensura de gratibus luminis, colorum umbrae*. Eberhard Klett, Augsburg (1760)
53. Lee, A.B., Pedersen, K.S., Mumford, D.: The nonlinear statistics of high-contrast patches in natural images. *Int. J. Comput. Vis.* **54**(1-3), 83–103 (2003)
54. Levine, Z.H., Kalukin, A.R., Kuhn, M., Retchi, C.C., Frigo, P., McNulty, I., Wang, Y., Lucatorto, T.B., Ravel, B.D., Tarrío, C.: Tomography of integrated circuit interconnect with an electromigration void. *J. Appl. Phys.* **87**(9), 4483–4488 (2000)
55. Li, S.Z.: *Markov random field modeling in computer vision*. Springer, London, (1995)
56. Li, G., Xi, N., Yu, M., Fung, W.-K.: Development of augmented reality system for afm-based nanomanipulation. *IEEE/ASME Trans. Mech.* **9**(2), 358–365 (2004)
57. Lucic, V., Forster, F., Baumeister, W.: Structural studies by electron tomography: from cells to molecules. *Annu. Rev. Biochem.* **74**, 833–865 (2005)
58. Mallick, S.P., Xu, Y., Kriegman, D.J.: Detecting particles in cryo-em micrographs using learned features. *J. Struct. Biol.* **145**(1-2), 52–62 (2004)
59. Mantooth, B.A., Donhauser, Z.J., Kelly, K.F., Weiss, P.S.: Cross-correlation image tracking for drift correction and adsorbate analysis. *Rev. Sci. Instrum.* **73**, 313–317 (2002)
60. Marco, S., Boudier, T., Messaoudi, C., Rigaud, J.-L.: Electron tomography of biological samples. *Biochemistry (Moscow)* **69**(11), 1219–1225 (2004)
61. McLachlan, G.J., Peel, D.: Robust cluster analysis via mixtures of multivariate t-distributions. In: *SSPR/SPR*, pp. 658–666 (1998)
62. Nicholson, W.V., Glaeser, R.M.: Review: automatic particle detection in electron microscopy. *J. Struct. Biol.* **133**, 90–101 (2001)
63. Nicholson, W.V., Malladi, R.: Correlation-based methods of automatic particle detection in electron microscopy images with smoothing by anisotropic diffusion. *J. Microsc.* **213**, 119–128 (2004)
64. NSRG-Chappel Hill: Nanoscale-Science Research Group. <http://www.cs.unc.edu/Research/nano/> (2005)
65. Ogura, T., Sato, C.: An automatic particle pickup method using a neural network applicable to low-contrast electron micrographs. *J. Struct. Biol.* **136**(3), 227–238 (2001)
66. Ong, E.W., Razdan, A., Garcia, A.A., Pizziconi, V.B., Ramakrishna, B.L., Glaunsinger, W.S.: Interactive nano-visualization of materials over the internet. *J. Chem. Educa.* **77**(9), 1114–1115 (2000)
67. Perona, P., Malik, J.: Scale-space and edge detection using anisotropic diffusion. *IEEE Trans. Pattern Anal. Mach. Intell.* **12**(7), 629–639 (1990)

68. Pohl, D.W.: Scanning near-field optical microscopy. *Advances in Optical and Electron Microscopy*. In: Sheppard, C.J.R., Mulvey, T., (eds.) Vol. 12. Academic, London (1990)
69. Ronneberger, O., Schultz, E., Burkhardt, H.: Automated pollen recognition using 3D volume images from fluorescence microscopy. *Aerobiologia* **18**(2), 107–115 (2002)
70. Rosenfeld, A., Pfaltz, J.: Distance functions on digital pictures. *Pattern Recogn* **1**(1), 33–61 July (1968)
71. Rugar, D., Budakian, R., Mamin, H.J., Chui, B.W.: Single spin detection by magnetic resonance force microscopy. *Nature*, 430, 329–332, July (2004)
72. Russ, J.C.: *The Image Processing Handbook*. IEEE Press, New York (1998)
73. Ryu, J., Horn, B.K.P., Mermelstein, M.S., Hong, S., Freedom, D.M.: Application of structured illumination in nanoscale vision. In: *Proceedings of IEEE Computer Society Conference on Computer Vision and Pattern Recognition Workshop: Computer Vision for the Nano Scale*, pp. 17–24, June (2003)
74. Sandberg, K., Mastrorade, D.N., Beylkina, G.: A fast reconstruction algorithm for electron microscope tomography. *J. Struct. Biol.* **144**, 61–72 (2003)
75. Scharf, H., Black, M., Haussecker, H.: Image statistics and anisotropic diffusion. In: *ICCV03*, pp. 840–847 (2003)
76. Scharf, H., Felsberg, M., Forssén, P.-E.: Noise adaptive channel smoothing of low-dose images. In: *Proceedings of IEEE computer society conference on computer vision and pattern recognition workshop: computer vision for the nano scale*, June (2003)
77. Scharf, H., Uttenweiler, D.: 3D anisotropic diffusion filtering for enhancing noisy actin filament fluorescence images. In: *Proceedings of the 23rd DAGM-symposium on pattern recognition*, pp. 69–75. Springer, London, (2001)
78. Sharma, G., Mavroidis, C., Ferreira, A.: Virtual reality and haptics in nano and bionanotechnology, vol. X of *Handbook of Theoretical and Computational Nanotechnology*, chap. 40. American Scientific Publishers, Stevenson Ranch (2005)
79. Singh, V., Marinescu, D.C., Baker, T.S.: Image segmentation for automatic particle identification in electron micrographs based on hidden markov random field models and expectation maximization. *J. Struct. Biol.* **145**(1-2), 123–141 (2004)
80. Stoscherk, A., Hegerl, R.: Automated detection of macromolecules from electron micrographs using advanced filter techniques. *J. Microsc.* **185**, 76–84 (1997)
81. Subramaniam, S., Milne, J.L.: Three-dimensional electron microscopy at molecular resolution. *Annu. Revi. Biophys. Biomol. Struct.* **33**, 141–155 (2004)
82. Tan, H.Z., Walker, L., Reifenberger, R., Mahadoo, S., Chiu, G., Raman, A., Helser, A., Colilla, P.: A haptic interface for human-in-the-loop manipulation at the nanoscale. In: *Proceedings of the 2005 world haptics conference (WHC05): the first joint euro haptics conference and the symposium on haptic interfaces for virtual environment and teleoperator systems*, pp. 271–276 (2005)
83. Tsai, R.Y.: A versatile camera calibration technique for high-accuracy 3D machine vision metrology using off-the-shelf TV cameras and lenses. *IEEE J. Robot. Autom.* **RA-3**(4), 323–344 (1987)
84. Valinetti, A., Fusiello, A., Murino, V.: Model tracking for video-based virtual reality. In: *ICIAAP*, pp. 372–377 (2001)
85. van Heel, M., Gowen, B., Matadeen, R., Orlova, E.V., Finn, R., Pape, T., Cohen, D., Stark, H., Schmidt, R., Schatz, M., Patwardhan, A.: Single-particle electron cryo-microscopy: towards atomic resolution. *Q.Revi. Biophys.* **33**(4), 307–369 (2000)
86. Viola, P., Jones, M.J.: Robust real-time face detection. *Int. J. Comput. Vis.* **57**(2), 137–154 (2004)
87. Watt, I.M.: *The Principles and Practice of Electron Microscopy*. Cambridge Press, Cambridge (1997)
88. Weickert, J.: *Anisotropic Diffusion in Image Processing*. Teubner Verlag, Stuttgart (1997)
89. Xiao, J., Shah, M.: Tri-view morphing. *Comput. Vis, Image Understand.* **96**(3), 345–366 (2004)
90. Yilmaz, A., Shafique, K., Shah, M.: Target tracking in airborne forward looking infrared imagery. *Image Vis. Comput.* **21**(7), 623–635 (2003)
91. Yu, Z., Bajaj, C.: A gravitation-based clustering method and its applications in 3D electron microscopy imaging. In: *5th International conference on advances in pattern recognition (ICAPR'03)*, pp. 137–140 (2003)
92. Yu, Z., Bajaj, C.: Detecting circular and rectangular particles based on geometric feature detection in electron micrographs. *J. Struct. Biol.* **145**, 168D180 (2004)
93. Zhang, Z.: A flexible new technique for camera calibration. *IEEE Trans. Pattern Anal. Mach. Intell.* **22**(11), 1330–1334 (2000)
94. Zhu, Y., Carragher, B., Kriegman, D., Milligan, R.A., Potter, C.S.: Automated identification of filaments in cryoelectron microscopy images. *J. Struct. Biol.* **135**, 302–321 (2001)
95. Zhu, Y., Carragher, B., Mouche, F., Potter, C.S.: Automatic particle detection through efficient Hough transforms. *IEEE Trans Med Imag.* **22**(9), 1053–1062 (2003)
96. Zhu, Y., Carragher, B., Glaeser, R.M., Fellmann, D., Bajaj, C., Bern, M., Mouche, F., de Haas, F., Hall, R. J., Kriegman, D.J., Ludtke, S.C., Mallick, S. P., Penczek, P.A., Roseman, A.M., Sigworth, F.J., Volkman, N., Potter, C.S.: Automatic particle selection: Results of a comparative study. *J. Struct. Biol.* **145**, 3–14 (2004)